IJISET - International Journal of Innovative Science, Engineering & Technology, Vol. 12 Issue 04, April 2025
ISSN (Online) 2348 – 7968 | Impact Factor – 6.72
www.ijiset.com

Characterization of Semiconductor Thin-Film Materials Using a Developed Microcontroller-Based Conductivity Measuring Device

O. I. Olusola[1], T. A. Obagade[2], M. D. Echendu[3], and O. A. Layioye[4]

[1]Condensed Matter and Statistical Physics Research Unit, Department of Physics, School of Physical Sciences, The Federal University of Technology, Akure (FUTA), P.M.B. 704, Nigeria.
Email: oiolusola@futa.edu.ng / olajideibk@yahoo.com

[2]Electronic Measurements and Instrumentation Research Unit, Department of Physics, School of Physical Sciences, The Federal University of Technology, Akure (FUTA), P.M.B. 704, Nigeria.
Email: taobagade@futa.edu.ng

[3]Electronic Measurements and Instrumentation Research Unit, Department of Physics, School of Physical Sciences, The Federal University of Technology, Akure (FUTA), P.M.B. 704, Nigeria.
Email: marizudaniel2006@gmail.com

[4]Electronic and Communication Research Unit, Department of Physics, School of Physical Sciences, The Federal University of Technology, Akure (FUTA), P.M.B. 704, Nigeria.
Email: oalayioye@futa.edu.ng

ABSTRACT

This study presents the characterization of semiconductor thin-film materials using a developed microcontroller-based conductivity measuring device. The device utilizes a four-wires probe technique to measure the electrical conductivity of semiconductor materials, and a microcontroller as a signal processor to monitor the measurement process and calculate the conductivity. The device also comprises a 5V DC regulated power supply, a constant current source, a gain amplifier, a signal processor, a liquid crystal display (LCD), a data logger. The device was used to characterize the conductivity of zinc telluride (ZnTe), magnessium copper seleride (MgCuSe), copper molybdenum telluride (CuMoTe), and cadmium manganese telluride (CdMnTe). The results of the measured conductivity values were in good agreement with the expected values based on the literature. The developed device provides a valuable tool to characterize the electrical properties of semiconductor thin-films, and has potential applications in research and development of electronic components.

KEYWORDS: *Four-points probe, Conductivity, Arduino-microcontroller, Semiconductors, Current, Voltage.*

1. INTRODUCTION

Conductivity, a property of materials that describe their ability to conduct electric current, heat, or other forms of energy has increasingly become an area of interest to researchers for decades, as it plays a crucial role in various fields and applications. So, measuring the conductivity of materials such as that of semiconductors is on the rise to immense heights in the field of semiconductor technology. (Obagade and Olusola, 2019), revealed that understanding the conductivity properties of semiconductor materials has helped in the development of advanced electronic components with improved performance. The conductivity of semiconductor thin-films has been a popular topic of discussion over time as it helps to understand the behaviours of semiconductor materials, predict their performance and optimize their suitability for different applications. (Garg *et al*., 2010) opined that measuring the conductivity of materials in many cases aids in understanding how semiconductor materials behaves over a range of different temperatures, which is vital for thermal management in electronics devices. However, (Lurz *et al.*, 2011) reported that identifying variations in conductivity has been a pivotal parameter in the design and fabrication of electronic devices and also, a means of detecting defects or impurities in the semiconductor materials, which may affect the performance of electronic components. (Boston *et al.*, 2017) revealed that accurate measurement of conductivity is an indispensable tool for characterizing, optimizing, and ensuring the reliability of semiconductor materials.

The measurement of semiconductor thin-film conductivity involves the use of many different techniques, including two-points probe technique, four-points probe technique, inductive (toroidal) conductivity probe technique, Van der Pauw technique, among others. According to (Seng *et al*., 2014), only two of these techniques; the two-points probe

and four-points probe techniques are the most commonly ones used to measure the properties of semiconductor thin-film materials. The two-points probe method, employs two electrodes to inject current unto the material in contact and also to measure voltage drop across the material. (Seng *et al*., 2014) reported that the two-points probe method is identified to be less accurate in performance, especially for use in semiconductor thin-films with relatively high conductivity. This is because the method uses direct and strong current as both the current and voltage leads are not separated. Also, this method may sometimes introduce contact resistances between the metal probes and semiconductor materials, which may easily destroy or alters the properties of the thin-film materials and this can significantly affect the measured voltage, leading to erroneous conductivity calculations. Therefore, to obtain more accurate conductivity values for semiconductor thin-films, studies such as (Panta and Subedi, 2012; Seng *et al*., 2014) revealed that the four-points probe technique, also known as four-points wire or four-points terminal is the best technique for measuring the conductivity values of materials.

This four-points probe technique employs four equally spaced electrodes in contact with a material of unknown resistance. This method enhances better accuracy of conductivity measurements especially in semiconductor films by minimizing the errors caused by contact resistances and the strong current associated with two-points probe technique; thus, ensuring uniform current distribution, leading to more reliable conductivity values (Seng *et al*., 2014, Waldrip *et al*., 2020). In view of the importance of conductivity measurement in studying the materials' behaviours, several studies have been conducted on this area and reviews of some relevant literatures in the present work are discussed. (Garg *et al*., 2010) employed a four-probe method to measure energy band-gap of a semiconductor sample, germanium. The results of the study showed that the resistivity values of the semiconductor samples decrease with increase in temperature, verifying the relationship between resistivity and temperature of semiconductors.

(Obagade and Olusola, 2019) developed a microcontroller-based conductivity measurement device to study the electrical properties of semiconductor thin-films. The results obtained showed that the device worked satisfactorily in determining both resistivity and conductivity of materials such as that of semiconductor thin-film materials using four-wires probe. (Palasantzas et al., 2000) worked on electrical conductivity of the thin-film growth dynamics. The results of the experiment revealed that different growth modes affect the conductivity behaviour of growing thin-film materials. (Panta and Subedi, 2012) carried out electrical characterization of aluminum (Al) thin films using four-point probe method. The results showed that resistivity of the film decreases linearly with increase in the film thickness. (Rajendran and Neelamegam, 2004) designed and developed a microcontroller-based conductivity measurement system. The comparative study of the device with other conductivity devices such as that of systronics conductivity meter showed that the device had good agreement with other convectional conductivity meters, proving the reliability of the device to measure conductivity of materials. (Reverter, 2022) proposes a microcontroller-based interface circuit for three-wire connected resistive sensors for the sake of making precise and accurate measurement. The result of the study revealed the vast potential of microcontroller-based systems in developing instrumentation is effective and reliable. (Seng *et al*., 2014) developed a custom-built conductivity measuring device for thin-film semiconductors and its application to polypyrrole. The comparative study of the conductivity values measured by the device with that of the standard type showed that the device has a good performance to determine the electrical conductivity of semiconductor materials.

So, as the measurement of conductivity became one of the most in-demand to characterize the behaviours of solid materials and also, in an effort to make it easy and possible to measure the conductivity of materials, it is necessary to develop an efficient and simple device that can accurately measure the electrical conductivity of materials, typically semiconductor. In this scenario, this work has developed a cost-effective microcontroller-based device using a four-points probe technique to characterize semiconductor materials.

2. MATERIALS AND METHODS

2.1 The Design Architecture of the Developed Device

The block diagram of design architecture of the device is shown in Figure 1, which illustrates the integration of hardware components and the data flow from the probe point to the display and storage units. The device is composed of eight units: a 5V DC regulated power supply, a constant current source, a current sensing unit, an amplification unit, a signal processing unit, a display unit, a storage unit, and a probing unit. A detailed explanation of the circuit design for each unit is provided in the following sections.

ISSN (Online) 2348 – 7968 | Impact Factor – 6.72

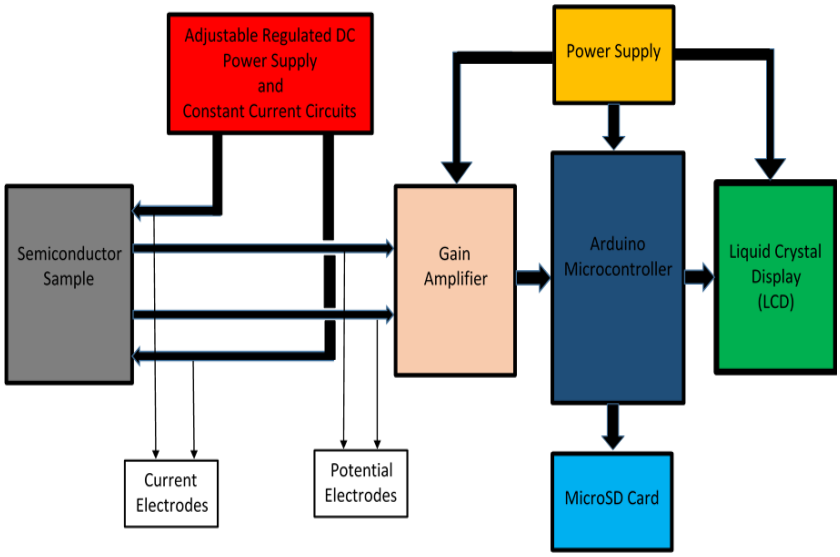

Figure 1: Block Diagram of the Developed Device

2.2 Direct Current (DC) Regulated Power Supply Circuit

An adjustable 5V DC regulated power supply was designed to provide electric current to semiconductor materials through a constant current circuit. It converts AC power from the mains into a stable DC voltage required by the constant current circuit. The power supply utilizes an LM7805 integrated circuit (IC) to achieve the necessary regulated DC output. A 12V step-down transformer reduces the high AC voltage to a lower AC voltage, which is then converted into DC by a bridge rectifier composed of four 1N4007 diodes. To eliminate ripples and ensure a smooth power supply, 470 µF and 10 µF decoupling capacitors are placed at the input and output of the circuit, respectively. A 1 kΩ potentiometer connected across the power supply output allows for voltage level adjustments. This power supply serves as the primary source for the device's constant current circuit. Figures 2a and 2b show the schematic diagram and pictorial view of the power supply circuit.

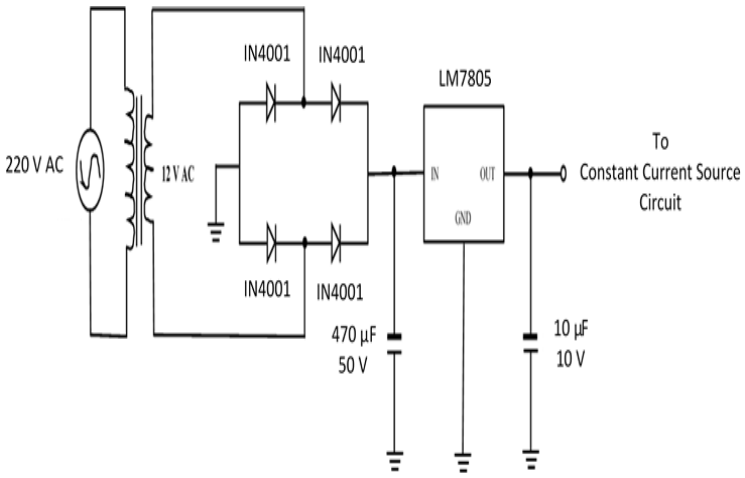

(a)

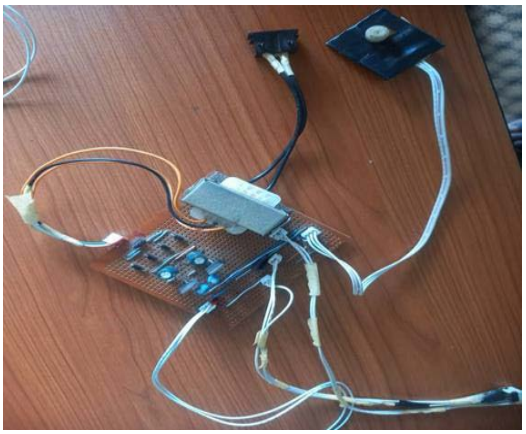

(b)

Figure 2: (a) Schematic circuit diagram of the 5 V power supply and (b) Pictorial view of the 5 V power supply circuit.

2.3 Constant Current Source Circuit

For accurate measurement of conductivity values of materials, a constant current source circuit is usually required as this circuit helps to provide a constant to the semiconductor material under test current even if there are any changes in the material's resistance or the supply voltage. In this work, this circuit was built around the MJ2955, a high-power transistor, and LM317, an adjustable voltage regulator to maintain a constant current output. The transistor MJ2955 acts as a pass transistor that is controlled by the voltage regulator LM317. The emitter of the transistor is connected to the voltage source from the output of the 5 V DC power supply circuit and the base of the transistor is connected to the input (Vin) of the voltage regulator as shown in Figure 3a.
The circuit works in such that the LM317 sets the emitter-base current of the transistor and this controls the emitter-collector current that flows through the transistor. The collector of the transistor is connected to the outer electrodes of the probe resistor to pass current into the load (semiconductor sample) and the voltage drop across the sample is measured through the inner electrodes of the probe. Figure 3b show the pictorial view of the constant current circuit.

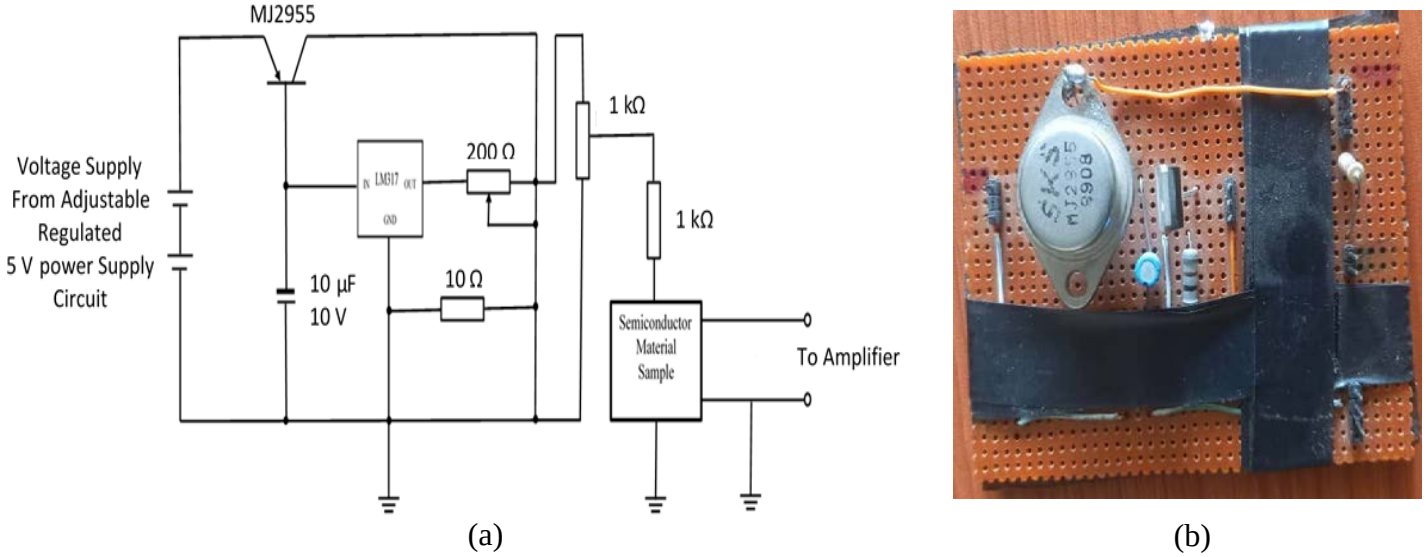

Figure 3: (a) Schematic circuit diagram of the 5 V power supply and (b) Pictorial view of the 5 V power supply circuit

2.4 The Four-Point Probe

The probe point for the device is a four-point probe that is often used to measure the electrical resistivity or conductivity of a material. It consists of four sharps, pointed electrodes that are collinearly arranged with equal spacing of 4 mm (0.4 cm) between them using a Schlumberger's arrays as shown in Figure 4a. The probe works by passing a current from the constant current circuit into a semiconductor material through the two outer electrodes (current electrodes), causing an induced voltage across the semiconductor sample. The induced voltage is measured by the two inner electrodes (potential electrodes). This voltage is most often very small; thus, it is required to be amplified before being passed to the microcontroller for further processing. Figure 4b show the pictorial view of the four-points probe.

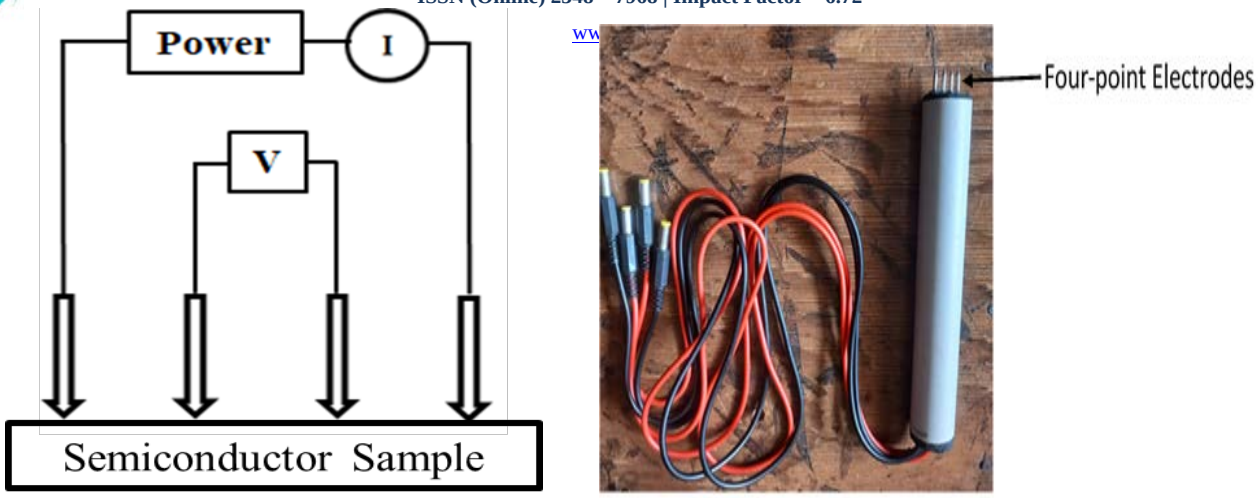

Figure 4: (a) The Schematic Arrangement of the four-points probe and (b) Pictorial view of the four-points probe

2.5 Gain Amplifier

The gain amplifier used for the amplification process of the voltage obtained across the semiconductor sample is a two stages non-inverting amplifier. The amplifier was built using two operational amplifiers (op-amps), LM741, a general-purpose op-amp with four resistive elements (R1, R2, R3 and R4) as depicted in Figure 5a. The input voltage to the amplifier is the voltage obtained from the semiconductor material through the probe. The circuit amplifies the voltage difference between the two input terminals of the operational amplifier to generate an output voltage. The amplifier's gain is calculated using the formula in Equation 1, while the output voltage is determined using the formula in Equation 2. Figure 5b show the pictorial view of the amplifier.

$$A_V = \left(1+\frac{R_2}{R_1}\right)\left(1+\frac{R_4}{R_3}\right) \tag{1}$$

$$V_{out} = \left(1+\frac{R_2}{R_1}\right)\left(1+\frac{R_4}{R_3}\right)\times V_{in} \tag{2}$$

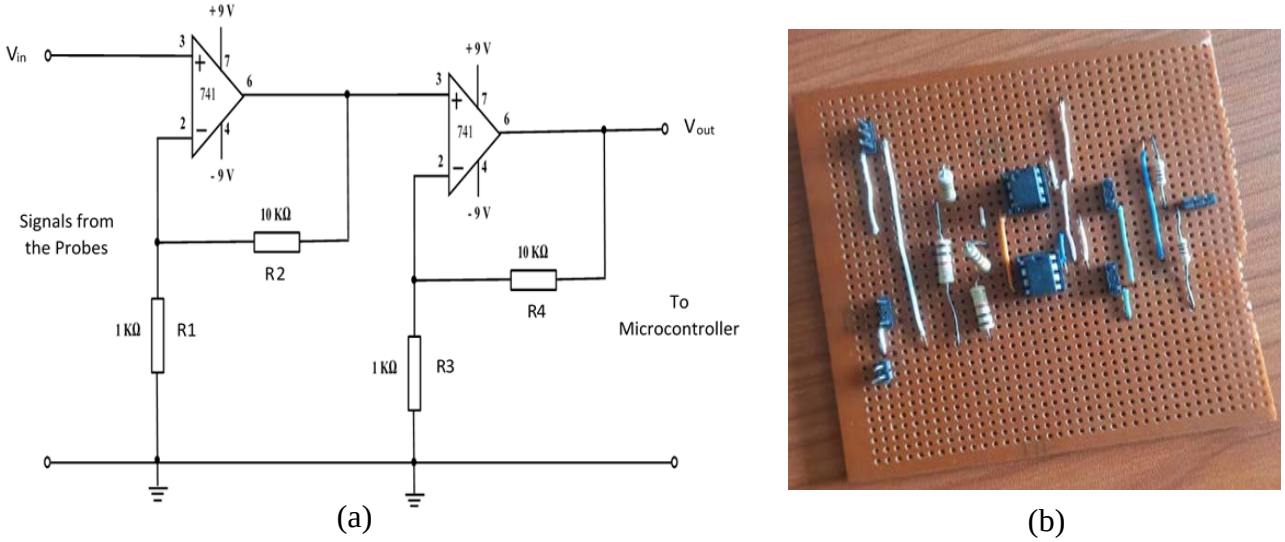

Figure 5: (a) The schematic circuit diagram of the gain amplifier and (b) Pictorial view of the gain amplifier

2.6 Signal Processor

The signal processor used in this device for the processing of output voltage from the amplifier is Arduino Uno microcontroller. The microcontroller was chosen based on its user-friendly feature and economic benefits. The microcontroller features an Atmega328P processor and is specifically designed for embedded applications, unlike microprocessors which are typically used in personal computers and general-purpose systems. It is an open-source hardware device featuring a low-power, 8-bit CMOS microcontroller based on AVR enhanced RISC architecture. While sharing common characteristics with other Arduino boards, it offers 14 digital input/output pins, including 6 that support Pulse Width Modulation (PWM), along with 6 analog input pins for reading analog signals. Additionally, it is equipped with a 16 MHz crystal oscillator, a USB interface, ICSP pins, a reset button, and a power jack. The microcontroller incorporates a 10-bit Analog-to-Digital Converter (ADC), 32 KB of Flash memory, 2 KB of SRAM, and 1 KB of EEPROM. Several digital pins also provide additional functionalities such as UART serial communication, SPI, I2C, and six interrupt lines. Programmed using the Arduino Integrated Development Environment (IDE) with C++, it processes analog voltage signals from the amplifier by converting them into digital values via its 10-bit ADC. Operating within a voltage range of 5V to 12V, it features a built-in voltage regulator that supplies both 3.3V and 5V to power other connected components. Figure 6 illustrates the Arduino Uno microcontroller.

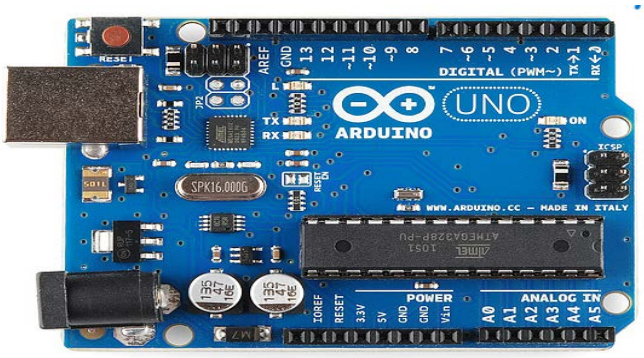

Figure 6: Arduino Uno Microcontroller Board

2.7 Output Display Screen

The output display used in this study to show the measured current and voltage values from the semiconductor's surface is a 20-character, 4-line Hitachi HD44780 Liquid Crystal Display (LCD) module. The LCD has 16 pins as shown in Figure 7, and these pins can be connected to the microcontroller in either 8-bit or 4-bit mode. In this work, the LCD is connected in 4-bit mode, utilizing only 6 of the LCD's pins for the connection to the microcontroller. The LCD can be powered with a maximum voltage of +7V, but in this case, it is powered with +5V from the microcontroller's generic power output.

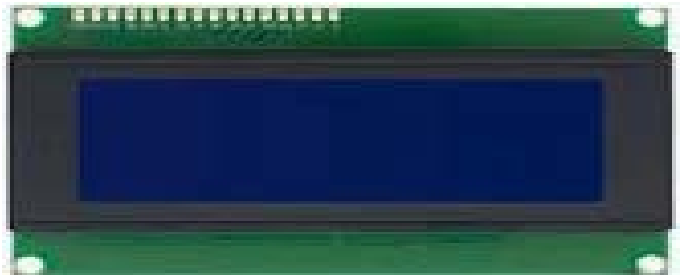

Figure 7: 20 x 4 Liquid Crystal Display (LCD)

2.8 Data Logger

The data logger is responsible for recording the conductivity measurements obtained from the developed device. It comprises a Secure Data (SD) card shield adapter/reader, manufactured by Seed Technology Incorporated, along with a microSD flash memory card. This setup allows data to be written to and retrieved from the card when inserted into the shield reader. The microSD flash memory card serves as a non-volatile storage medium. Communication between the card shield reader and the microcontroller is facilitated through the Serial Peripheral Interface (SPI) protocol, enabling continuous data storage on the microSD card over time. The data is stored in a plain Excel file format on the SD card, which can be downloaded to a computer for further analysis. Figure 8 illustrates the interfacing procedure of the microSD card with the microcontroller board.

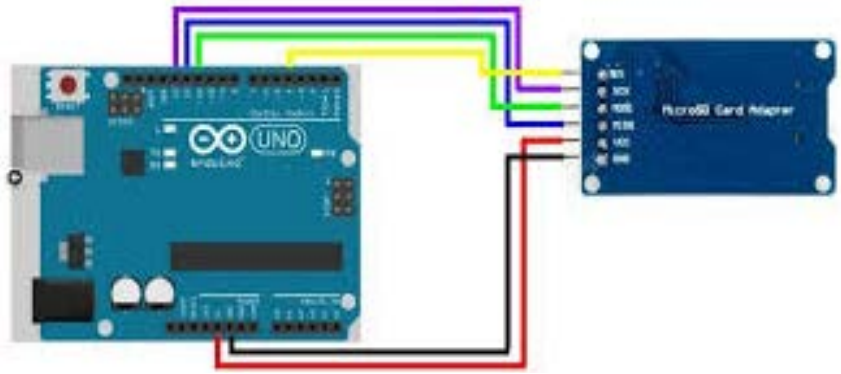

Figure 8: Connection of MicroSD Card Module with Arduino Uno Microcontroller Board

2.9 Power Supply

The system was powered by a +9V lithium battery connected through the voltage input pin (Vin) of the Arduino microcontroller. Other components, including the LCD and microSD card shield, received a +5V power supply. The amplification circuits also operated within this voltage range, which was sourced from the standard power output terminals on the Arduino microcontroller board.

3. EXPERIMENTAL SETUP

An experiment was carried out to evaluate the performance, reliability, and accuracy of the developed device by comparing its results with experimental data. In the setup, a regulated 5V DC supply, derived from an alternating current (AC) mains source, was used to pass current through the semiconductor sample, as illustrated in Figure 9.
To prevent excessive current from flowing into the sample, a fixed 1 kΩ resistor was incorporated into the circuit to regulate the current flow. Two digital multimeters were employed as indicated in the arrangement; one of the meters was used as an ammeter A, to detect the current being passed into the semiconductor sample and the second meter was used as a voltmeter V, to measure the voltage being induced on the surface of the sample.

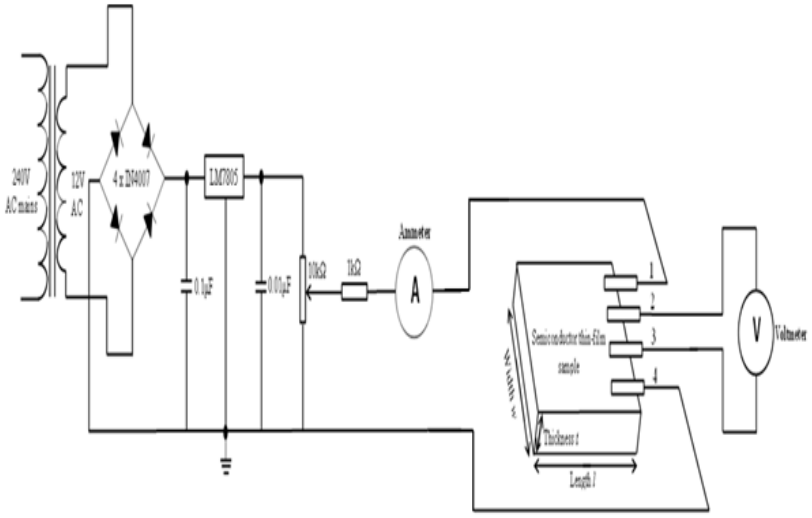

Figure 9: Schematic Diagram of the Experimental Setup

3.1 Test and Calibration of the Device

Each component of the developed device was tested individually to verify its proper functionality and ensure the reliability of the data produced before assembling them together. The entire coupled device was tested by measuring the conductivity of cadmium telluride (CdTe) semiconductor thin-film sample, and in the testing procedure, an experimental setup discussed in the preceding section was equally used to carry out conductivity measurement of the same semiconductor sample alongside the developed device and the result of the measurement is shown in Table 1. The result obtained was used to calibrate the developed device by carrying out some adjustments on the instruction codes of the software unit of the device. After necessary adjustments, the device was used to carry out conductivity measurements of four different semiconductor samples, namely: zinc telluride (ZnTe), magnessium copper seleride (MgCuSe), copper molybdenum telluride (CuMoTe), and cadmium manganese telluride (CdMnTe) to test for the functionality and performance of the developed device. The results of the measurements are presented in Tables 2-5 in the following section.

4. RESULTS AND DISCUSSION

4.1 Performance Evaluation of the Developed Device

The performance of the device as presented in Table 1 was evaluated by comparing the two sets of voltages measured by the device and the standard experimental setup. In the comparative study, a correlation analysis being a method of statistical technique for assessing the strength of relationships between two or more variables was conducted. A linear fit plot of the voltage values was generated, as illustrated in Figure 10. The plot demonstrated a strong linear correlation ($R^2 = 1$), signifying a perfect relationship. This demonstrates that the developed device performs well, with high accuracy and reliability. Four semiconductor samples were used to test the device. The measurements obtained from the developed device were compared with those from standard instruments, and the results are presented in Figures 11 to 14. The four semiconductors tested were zinc telluride (ZnTe), a binary compound semiconductor, and three ternary compound semiconductors: copper molybdenum telluride (CuMoTe), magnesium copper selenide (MgCuSe), and cadmium manganese telluride (CdMnTe). These materials are nearly identical in size and exhibit different behaviors, as shown in the current-voltage (I-V) characteristics in Figures 11 to 14.

Table 1: Voltage Measurements from the Developed Device and Standard Instrument

Voltage Measurement from Standard Instrument (V)	Voltage Measurement from Developed Device (V)
0.000	0.000
0.170	0.178
0.240	0.251
0.320	0.335
0.470	0.483
0.530	0.542
0.580	0.594
0.660	0.671
0.780	0.795
0.850	0.862
1.120	1.131
1.250	1.264
1.470	1.482
1.660	1.675
1.730	1.741
1.840	1.852
1.910	1.925
2.030	2.042
2.180	2.193
2.290	2.303
2.370	2.384

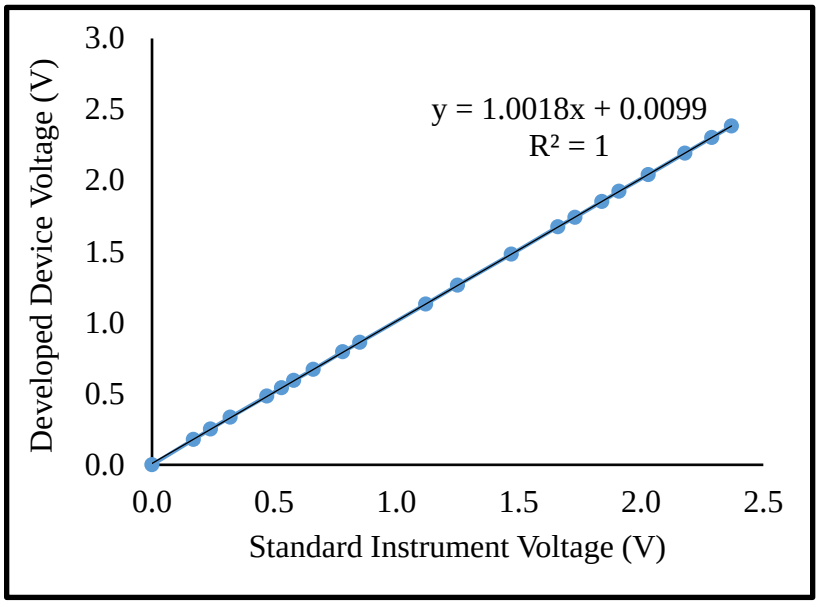

Figure 10: Trend of Voltages Measured by the Developed Device and the Standard Instrument

Table 2 show the results of current-voltage (I-V) measurement obtained from ZnTe semiconductor thin films using the developed device and the standard experimental setup. Figures 11a and 11b display I-V characteristic curves of the results respectively. The material's resistance, determined from the inverse slope of the curves, was 1682.69 Ω for the developed device and 1687.56 Ω for the standard setup. Correspondingly, the resistivity values were 155.65 Ωcm and 156.10 Ωcm, while the conductivity values were 0.00643 S/cm and 0.00641 S/cm, respectively. The deviation in conductivity values falls within ±0.00002 S/cm, which is negligible.

Table 2: Result of Current-Voltage (I-V) Measurement from ZnTe Sample

Developed Device Reading		Standard Instrument Reading	
V (V)	I (mA)	V (V)	I (mA)
0.00	0.000	0.00	0.000
0.25	0.080	0.25	0.078
0.50	0.260	0.50	0.257
0.75	0.430	0.75	0.426
1.00	0.530	1.00	0.529
1.25	0.720	1.25	0.715
1.50	0.920	1.50	0.916
1.75	1.090	1.75	1.080
2.00	1.220	2.00	1.200
2.25	1.400	2.25	1.370
2.50	1.380	2.50	1.378
2.75	1.500	2.75	1.480
3.00	1.530	3.00	1.526
3.25	1.590	3.25	1.588
3.50	1.770	3.50	1.769
3.75	1.910	3.75	1.905
4.00	2.090	4.00	2.087
4.25	2.220	4.25	2.216
4.50	2.320	4.50	2.315
4.75	2.460	4.75	2.459
5.00	2.630	5.00	2.625

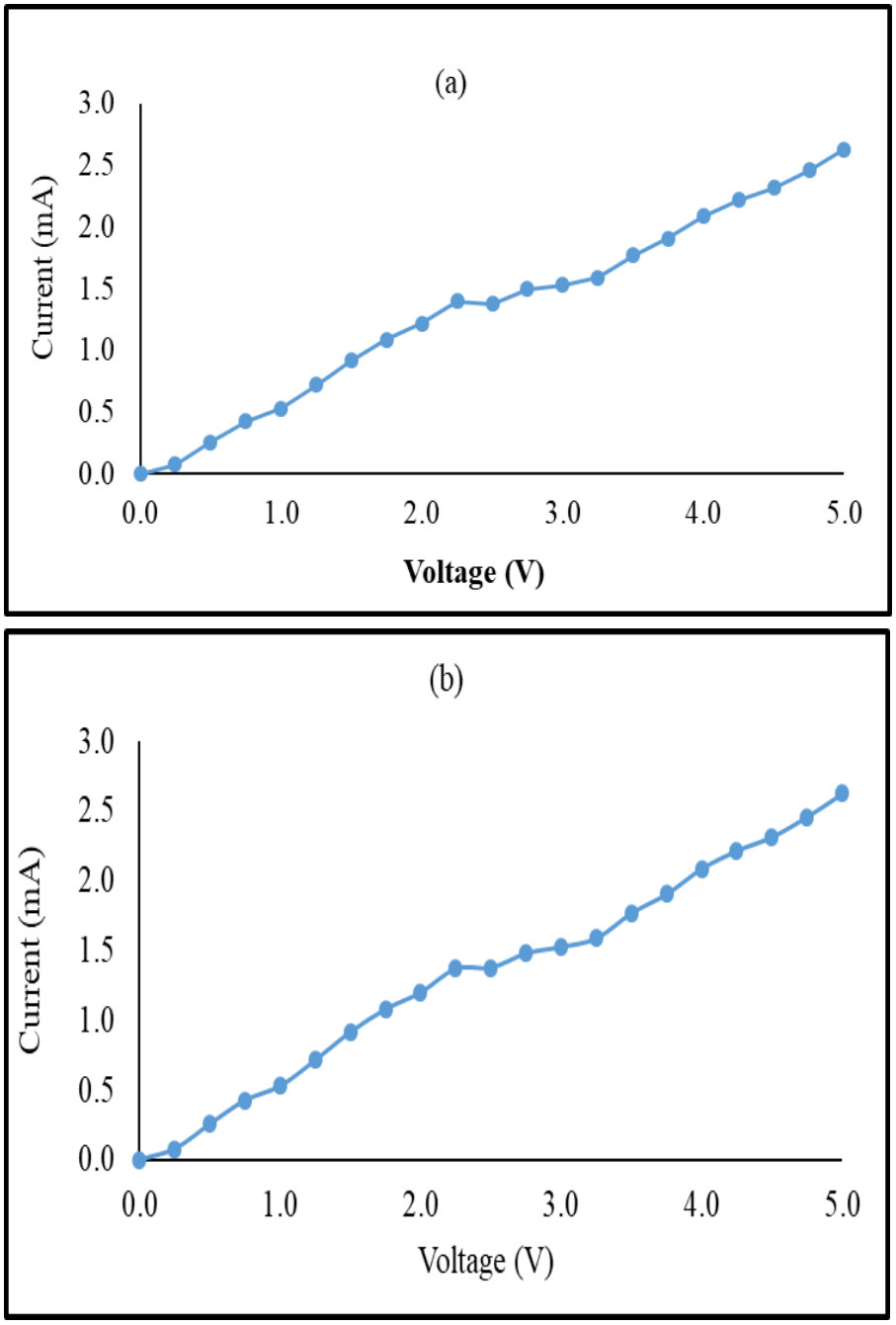

Figure 11: Current-Voltage (I-V) Characteristics of ZnTe Thin-films Obtained from (a) Developed device and (b) Standard experimental setup.

Table 3 show the results of current-voltage (I-V) measurement obtained from CuMoTe semiconductor thin films using the developed device and the standard experimental setup. Figures 12a and 12b display I-V characteristic curves of the results respectively. The resistance of the material as obtained from the slope inverse of the curves are 1923.08 Ω and 1920.97 Ω for the developed and standard setup respectively. In this view, the resistivities are 153.69 Ωcm and 153.52 Ωcm; and the conductivities are 0.00650 S/cm and 0.00651 S/cm respectively. The deviation between the conductivity values lies within the range ±0.00001 S/cm which is very insignificant.

Table 3: Result of Current-Voltage (I-V) Measurement from CuMoTe Sample

Developed Device Reading		Experimental Setup Reading	
V (V)	I (mA)	V (V)	I (mA)
0.00	0.000	0.00	0.000
0.25	0.210	0.25	0.206
0.50	0.410	0.50	0.408
0.75	0.630	0.75	0.625
1.00	0.640	1.00	0.638
1.25	0.590	1.25	0.586
1.50	0.510	1.50	0.508
1.75	0.730	1.75	0.727
2.00	0.850	2.00	0.849
2.25	1.030	2.25	1.026
2.50	1.110	2.50	1.108
2.75	1.270	2.75	1.265
3.00	1.450	3.00	1.446
3.25	1.620	3.25	1.618
3.50	1.730	3.50	1.729
3.75	1.860	3.75	1.858
4.00	1.990	4.00	1.987
4.25	2.110	4.25	2.106
4.50	2.290	4.50	2.288
4.75	2.440	4.75	2.437
5.00	2.530	5.00	2.529

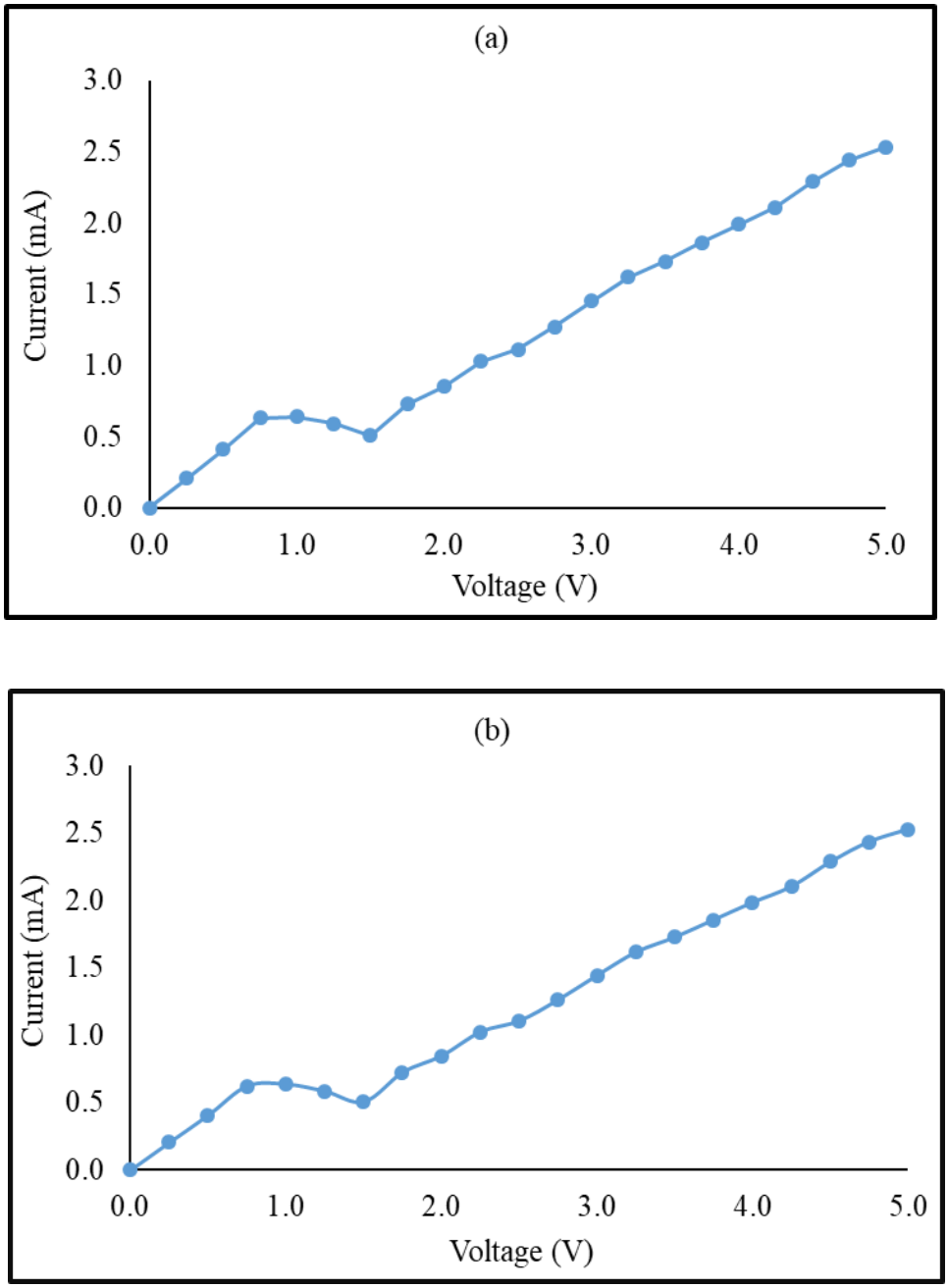

Figure 12: Current-voltage (I-V) Characteristics of CuMoTe Thin-films Obtained from (a) Developed device and (b) Standard experimental setup.

Table 4 show the results of current-voltage (I-V) measurement obtained from MgCuSe semiconductor thin films using the developed device and the standard experimental setup. Figures 13a and 13b display I-V characteristic curves of the results respectively. The resistance of the material as obtained from the slope inverse of the curves are 1750.00 Ω and 1748.25 Ω for the developed and standard setup respectively. In this view, the resistivities are 170.94 Ωcm and 170.77 Ωcm respectively; and the conductivities are 0.00585 S/cm and 0.00586 S/cm respectively. The deviation between the conductivity values also lies within the range ±0.00001 S/cm.

Table 4: Result of Current-Voltage (I-V) Measurement from MgCuSe sample

Developed Device Reading		Experimental Setup Reading	
V (V)	I (mA)	V (V)	I (mA)
0.00	0.000	0.00	0.000
0.25	0.170	0.25	0.168
0.50	0.330	0.50	0.325
0.75	0.460	0.75	0.457
1.00	0.570	1.00	0.568
1.25	0.700	1.25	0.680
1.50	0.770	1.50	0.767
1.75	0.860	1.75	0.859
2.00	1.040	2.00	1.030
2.25	1.140	2.25	1.136
2.50	1.160	2.50	1.157
2.75	1.330	2.75	1.325
3.00	1.490	3.00	1.488
3.25	1.620	3.25	1.616
3.50	1.780	3.50	1.779
3.75	1.960	3.75	1.958
4.00	2.120	4.00	2.115
4.25	2.290	4.25	2.285
4.50	2.430	4.50	2.426
4.75	2.540	4.75	2.538
5.00	2.620	5.00	2.617

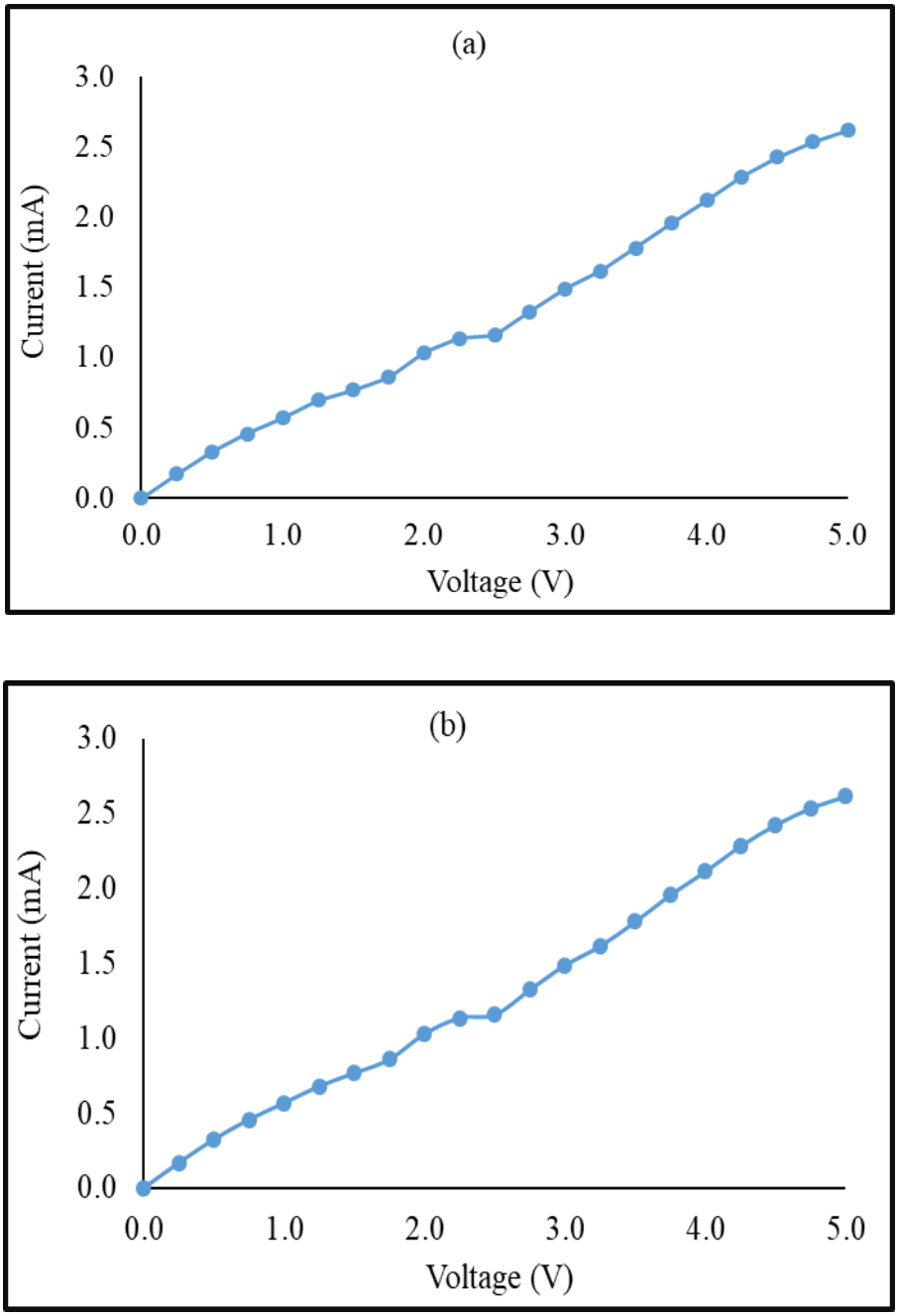

Figure 13: Current-Voltage (I-V) Characteristics of MgCuSe Thin-films Obtained from (a) Developed device and (b) Standard experimental setup.

Table 5 show the results of current-voltage (I-V) measurement obtained from CdMnTe semiconductor thin films using the developed device and the standard experimental setup. Figures 14a and 14b display I-V characteristic curves of the results respectively. The material's resistance, determined from the inverse slope of the curves, was 1666.67 Ω for the developed device and 1669.85 Ω for the standard setup. Accordingly, the resistivity values were 185.00 Ωcm and 185.35 Ωcm, while the conductivity values were 0.00541 S/cm and 0.00540 S/cm, respectively. The deviation between these conductivity values is ±0.00001 S/cm, which is negligible.

Table 5: Result of current-voltage measurement from CdMnTe sample

Developed Device Reading		Experimental Setup Reading	
V (V)	I (mA)	V (V)	I (mA)
0.00	0.000	0.00	0.000
0.25	0.160	0.25	0.156
0.50	0.310	0.50	0.307
0.75	0.430	0.75	0.429
1.00	0.520	1.00	0.518
1.25	0.580	1.25	0.576
1.50	0.610	1.50	0.605
1.75	0.710	1.75	0.708
2.00	0.740	2.00	0.739
2.25	0.860	2.25	0.856
2.50	1.020	2.50	1.010
2.75	1.180	2.75	1.175
3.00	1.360	3.00	1.359
3.25	1.440	3.25	1.438
3.50	1.530	3.50	1.527
3.75	1.710	3.75	1.709
4.00	1.840	4.00	1.836
4.25	1.970	4.25	1.965
4.50	2.130	4.50	2.128
4.75	2.320	4.75	2.315
5.00	2.490	5.00	2.486

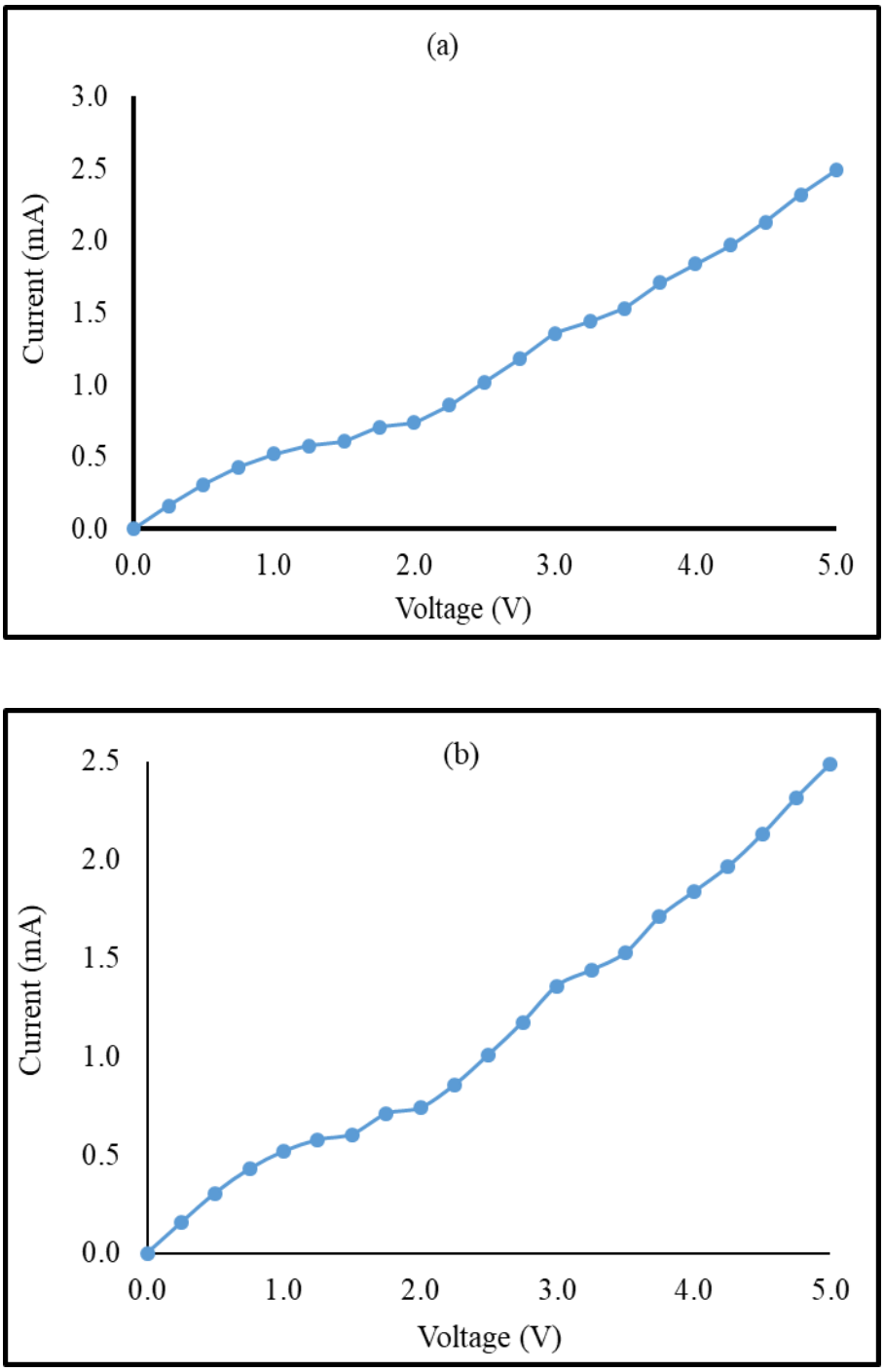

Figure 14: Current-Voltage (I-V) characteristics of CdMnTe thin films obtained from (a) Developed device and (b) Standard experimental setup.

From the results of resistivities and conductivities deduced from the four semiconductors used in carrying out the performance of the device, it was seen that that their electrical resistivities and conductivities are different. Also, from the current-voltage (I-V) characteristics illustrated in Figures 11 to 14, the materials showed different behaviours thus pointing to the distinct peculiarities possessed by each semiconductor material. Also, the resistivities obtained in this work is of the order of 10^2 and it falls within the possible range of resistivity values that semiconductor materials have. It has been reported that the resistivity value of semiconductor falls within the range of 10^{-4} to 10^8 Ωcm (Dharmadasa, 2013)

The results presented in Figures 11 to 14 also showed that the I-V characteristics are not perfectly linear; rather, they showed a non-linear response. This can be mainly attributed to factors such as the technique used during the thin film growth and the nature of the substrate used. One of such growth techniques which can cause a non-uniformity in the material doping is electrodeposition technique (Echendu and Dharmadasa, 2015).

The semiconductor materials used in this research for measurement purpose were grown using electrodeposition technique and glass/fluorine-doped tin oxide (FTO) substrate was used.

It has been reported that FTO substrates have rough and spiky surfaces. When power supply is turned on during electrodeposition, the electric field at the tip of the FTO spikes are higher in magnitude than the ones at the valley and these tips form the nucleation centre for the thin films molecule to grow. As the molecules are stacked against each other during growth, they tend to grow upwards at a perpendicular direction to the FTO surface.
This kind of columnar growth will create non-uniformity in the electrodeposited materials and sometimes, lead to pin holes formation (Salim *et al*., 2016).
The non-uniformity in the material doping causes the film thickness at the spiky surface to be different from the other substrate section (most especially the valley). The existence of non – uniform doping which arises as a result of electric field variations in the substrate surface is a major cause of non-linearity in the I-V response.

Also, the formation of pin holes which are also referred to as shunting paths can produce a shunt resistance. This shunt resistance creates a parallel resistance paths such as leakage currents which can also lead to the non – linearity in the I-V response. It should also be noted that the non-linear response observed in Figures 11 to 14 could arise as a result of non – idealities in the semiconductor materials such as impurities and defects.

5. CONCLUSION

This study introduces the design and development of a microcontroller-based device for measuring the conductivity of semiconductor thin-film materials. The results indicate that the device performed effectively, utilizing a four-point probe and Arduino microcontroller as the core components. Given its performance, the device could serve as an affordable alternative to the expensive conventional models available on the market, as it was constructed from low-cost, locally available materials. The device is suitable for use in laboratories for demonstration, research purposes, and in related industries. Its simple design makes it cost-effective and easier to maintain.

ACKNOWLEDGEMENT

The authors would like to thank The Federal University of Technology Akure (FUTA), Ondo State, Nigeria for providing the facilities required in implementing the research project.

DECLARATION OF COMPETING INTEREST

The authors declare that there are no competing interests.

FUNDING SOURCES

This research did not receive specific grants from any funding agencies.

REFERENCES

Boston, R., Schmidt, W. L., Lewin, G. D., Iyasara, A. C., Lu, Z., Zhang, H., and Reaney, I. M. "Protocols for the Fabrication, Characterization, and Optimization of N-type Thermoelectric Ceramic Oxides", *Chemistry of Materials*, 29 (1), 2017, 265-280.

Dharmadasa, I. M. Advances in Thin-Film Solar Cells (First ed.). Boulevard, Singapore: Pan Stanford Publishing Pte. Ltd, 2013.

Echendu, O. K., and Dharmadasa, I. M. "Graded-Bandgap Solar Cells Using Al-Electrodeposited ZnS, CdS and CdTe Thin-Films", *Energies*, 8 (5), 2015, 4416–4435.

Garg A., Sharma R., and Dhingra V. "Automating Energy Bandgap Measurements in Semiconductors Using LabVIEW", *European Journal of Physics Education*, 2010, 2-14.

Lutz, J., Schlangenotto, H., Scheuermann, U., and De Doncker, R. "Semiconductor power devices", *Physics, characteristics, reliability*, *2*. Second Edition: Springer International Publishing AG, 2011. ISBN 978-3-319-70916. https://doi.org/10.1007/978-3-319-70917-8

Obagade T. A., and Olusola O. I. "Development of a Microcontroller Based Conductivity Measurement Device for Semiconductor Thin-Films Application", *International Organization of Scientific Research Journal of Applied Physics*, 11(3), 2019, 38-44. DOI: 10.9790/4861-1103023844

Palasantzas, G., Zhao, Y. P., Wang, G. C., Lu, T. M., Barnas, J., and De Hosson, J. T. M. "Electrical conductivity and thin-film growth dynamics", *Physical Review Bulleting*, 61 (16), 2000, 11109.

Panta, G. P., and Subedi, D. P. "Electrical Characterization of Aluminum (Al) Thin-Films Measured by Using Four-Point Probe Method", *Kathmandu University journal of science, Engineering and Technology*, 8 (2), 2012, 31-36.

Rajendran, A., and Neelamegam, P. "Design and Development of Microcontroller-Based Conductivity Measurement System", *Indian Journal of Pure and Applied Physics (IJPAP)*, 42 (03), 2004. http://nopr.niscpr.res.in/handle/123456789/9572

Reverter, F. "A Microcontroller-Based Interface Circuit for Three-Wire Connected Resistive Sensors", *IEEE Transactions on Instrumentation and Measurement*, 71, 2022, 1-4.

Seng, S., Shinpei, T., Yoshihiko, I., and Masakazu, K. "Development of a Handmade Conductivity Measurement Device for a Thin-film Semiconductor and its Application to Polypyrrole", *Journal of Chemical Education*, 91(11), 2014, 1971-1975.

Waldrip, M., Jurchescu, O. D., Gundlach, D. J., and Bittle, E. G. "Contact Resistance in Organic Field Effect Transistors: Conquering the Barrier", *Advanced Functional Materials*, *30*(20), 2020, 1904576. https://doi.org/10.1002/adfm.201904576

Salim, H. I., Olusola, O. I., Ojo, A. A., Urasov, K. A., Dergacheva, M. B., and Dharmadasa, I. M. "Electrodeposition and Characterisation of CdS Thin Films using Thiourea Precursor for Application in Solar Cells", *Journal of Materials Science: Materials in Electronics*, *27*(7), 2016, 6786–6799. https://doi.org/10.1007/s10854-016-4629-8